Наносистеми, наноматеріали, нанотехнології
Nanosistemi, Nanomateriali, Nanotehnologii
2016, т. 14, № 4, сс. 527–537

PACS numbers: 43.35.Cg, 62.20.D-, 62.23.Pq, 62.65.+k, 68.65.Pq, 82.30.Lp, 83.80.Jx

Impact of Few-Layered Graphene Plates on Structure and Properties of an Epoxy Resin

B. M. Gorelov[1], A. M. Gorb[2], O. I. Polovina[2], A. B. Nadtochiy[2], D. L. Starokadomskiy[1], S. V. Shulga[3], and V. M. Ogenko[3]

[1]*O. O. Chuiko Institute of Surface Chemistry, N.A.S. of Ukraine, 17, General Naumov Str., 03164 Kyiv, Ukraine*
[2]*Taras Shevchenko Kyiv National University, Department of Physics, 64/13, Volodymyrska Str., 01601 Kyiv, Ukraine*
[3]*V. I. Vernadsky Institute of General and Inorganic Chemistry, N.A.S. of Ukraine 32–34, Academician Palladin Ave., 03142 Kyiv, Ukraine*

Impact of few-layered graphene (FLG) plates on the properties of the ED-20 epoxy resin is experimentally studied by using various techniques. The average dimensions of FLG plates are estimated as about 50 nm in thickness and 5 μm in both width and length. The FLG-mass-loading, C_f, in the nanocomposites is ranged from 0.01% to 5%. On the whole, the FLG plates promote an improvement in the thermal and chemical resistivities of the nanocomposites due to the chemical binding of the epoxy macromolecular chains to the free carbon bonds located on lateral verges of the plates. On the other hand, the FLG plates worsen the tensile strength of the nanocomposites at $C_f > 0.01\%$, whereas the dynamic elastic moduli undergo small variations.

З використанням різних методик експериментально досліджено вплив багатошарових графенових (БШГ) платівок на властивості епоксидної смоли ЕД-20. Середні розміри БШГ-платівок складали приблизно 5 мкм у довжину та ширину і 50 нм у товщину. Масове навантаження C_f БШГ-платівок у нанокомпозитах змінювалося від 0,01% до 5%. У цілому, БШГ-платівки спричиняють поліпшення як термічної, так і хемічної стійкости нанокомпозитів внаслідок хемічного зв'язування макромолекулярних ланцюжків смоли з вільними Карбоновими зв'язками, що локалізовані на бічних гранях платівок. З іншого боку, БШГ-платівки призводять до погіршення межі міцности нанокомпозитів за наповнень $C_f > 0{,}01\%$, хоча динамічні пружні модулі зазнають незначних змін.

С использованием различных методик экспериментально исследовано влияние многослойных графеновых (МСГ) пластинок на свойства эпоксидной смолы ЭД-20. Средние размеры МСГ-пластинок составляли примерно 5 мкм в длину и ширину и 50 нм по толщине. Массовая нагрузка C_f МСГ-пластинок в нанокомпозитах изменялась от 0,01% до 5%. В целом, МСГ-пластинки способствуют улучшению как термической, так и химической стойкости нанокомпозитов вследствие химического связывания макромолекулярных цепочек смолы со свободными углеродными связями, локализованными на боковых гранях пластинок. С другой стороны, МСГ-пластинки ухудшают предел разрушения нанокомпозитов при наполнениях $C_f > 0{,}01$, в то время как динамические упругие модули претерпевают незначительные изменения.

Key words: few-layer graphene, epoxy resin, nanocomposite, thermal decomposition, tensile strength, swell index.

Ключові слова: графен багатошаровий, смола епоксидна, нанокомпозит, деструкція термічна, межа міцности, показник набрякання.

Ключевые слова: графен многослойный, смола эпоксидная, деструкция термическая, предел прочности, показатель набухания.

(Received 30 November, 2016; in final version, 2 December, 2016)

1. INTRODUCTION

Today, efficient heat removal became a critical (crucial) issue for the performance and reliability of modern electronic, optoelectronic, photonic devices and systems [1]. As a consequence, thermal interface materials (TIMs) applied between heat sources and heat sinks are essential ingredients of thermal management. The unique mechanical, thermal, and charge-transport properties of graphene in addition to its extremely high surface area and gas impermeability [2] make graphene as promising nanosize filler for modifying molecular structure of polymers and, hence, for obtaining efficient TIMs.

Graphene is a single-atom-thick sheet of sp^2-hybridized carbon atoms tightly packed in a two-dimensional ($2D$) honeycomb lattice with a carbon-carbon distance of 0.142 nm [3–5]. It has theoretical value of a room temperature thermal conductivity of about 5000 $W \cdot m^{-1} \cdot K^{-1}$ [6, 7] higher than that of carbon nanotubes (3000–3500 $W \cdot m^{-1} \cdot K^{-1}$) [8] and diamond (2000 W·m·K) [9]. Recent experimental work on a large graphene membrane has shown the coefficient of thermal conductivity to be $\cong 600$ $W \cdot m^{-1} \cdot K^{-1}$ [10] that is several times higher than that of copper. This means that graphene is able to dissipate heat readily.

However, when expecting the graphene-filled PNCs to be efficient TIMs, it is necessary to understand how graphene will influence the thermal resistivity on every polymer matrix. Relatively low thermal

resistivity and thermal stability of 3*D*-network thermosetting polymers such as epoxy or polyester resins remain a key challenge for materials science due to an extremely wide area of their applications. Therefore, increasing the thermal resistivity of the resins by nanofillers enables to meet more severe heat-dissipation requirements for many plastics applications.

The few-layered graphene (FLG) particles, which consist of weakly coupled graphene layers, have recently been obtained [11]. The FLG particles expose strong anisotropy in their physical and chemical properties. The layers retain high values of both electro- and thermal conductivities inherent to the single graphene sheet. However, the conductivities drop by several orders of magnitude in a direction perpendicular to the layers. The lateral verges of FLG particles have high reactionary ability due to free carbon-bonds located on the edges of the layers. The basal planes are inert but may include a bit active surface sites due to structural defects. Therefore, the FLG particles being embedded into a polymer matrix may vary essentially its functional properties in either improvement or worsening of operation parameters.

Therefore, the aim of the present work is to study impact of such FLG particles on mechanical, thermal, and structural properties of an epoxy resin.

2. EXPERIMENTAL SECTION

2.1. The FLG Particles: Preparation and Structure

To prepare the FLG particles for our experiments, we started from the graphite scales, which have been obtained by using the technique described in [11]. The scales have been filtrated, washed first by distilled water and then by ethanol three times, and dried. The dry material has been dispersed (8 g/l) in boiling ethanol and treated by 20 kHz ultrasound until a steady suspension was formed. To prevent the FLG plates from oxidation, they have been kept as the suspension. The electronographic study showed the particles to be few-layered graphene of about 5×5 μm in plane dimensions and 50 nm in thickness (see Fig. 1). The X-ray diffraction analysis showed that the FLG plates contain about 40 single-atom-thick graphene sheets. It has earlier been shown that both the physical and chemical properties of the material do not vary if number of layers exceeds 3 [12].

2.2. Preparing the Composites

The epoxy resin ED-20 has been used to prepare the FLG filled

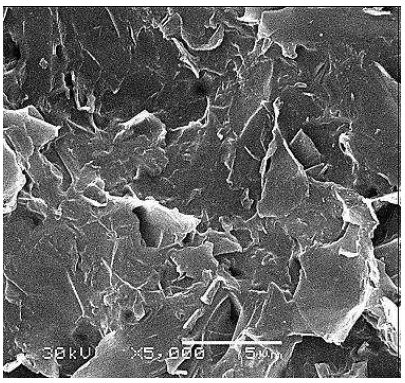

Fig. 1. TEM-photograph of FLG plates.

nanocomposites. The structural formula of the resin can be found elsewhere [13]. Here, we used PEPA as the hardener agent to cure both the initial oligomeric solution and correspondent mixtures filled with the FLG plates.

The FLG filled nanocomposites have been obtained by adding the suspension of a required graphene density into the initial oligomeric solution. The mixtures were cured during 72 hours at 24°C.

2.3. Experimental Techniques

The experimental studies have been carried out by using the programmable thermal desorption mass-spectroscopy (PTDMS), the static mechanical loading (SML), the ultrasound velocity measurements (USM), and swelling in the polygraph solvent.

The 'Shopper' testing machine has been used to compress the samples. The samples were cylinder-shaped of 10 mm in both height and diameter. The destruction strength (P) and the Young's modulus (E) have been determined as 5-samples-averaged values. The Poisson's ratio (ν) has been calculated by means of formula [14]

$$(1 + \nu) = E(1 - 2\nu) / 6\sigma_F ,$$

where σ_F is the fluidity limit.

The ultrasound-velocity measurements have been carried out by the phase-frequency technique in a continuous wave mode of operation [15] within the frequency range of 1.5–2.0 MHz where ultrasound vibrations suffer both negligible dispersion and high attenuation. The experimental details can be found elsewhere [16]. The relative errors in the longitudinal (V_L) and shear (V_S) elastic wave phase velocities did not exceed 0.7%.

Content of volatile products emanated by samples during its thermal decomposition has been determined by using a programmable thermal desorption technique combined with a mass-spectrometric detection [17, 18].

The samples for studying the swelling have been prepared as the tablets of 25 mm in diameter and 5 mm in thickness. The neutral polygraph solvent has been used as fluid media because it does not react chemically with the resin and is of high rate of penetration into the resin. The swelling have been studied at a room temperature.

3. RESULTS AND DISCUSSION

3.1. The Static Mechanical Loading

Under static mechanical loading, the tensile strength on a compression (P) decreases gradually with increasing loading. It is noticeable that decreasing P is accompanied with a weak increasing of the Young's modulus (E) (see Fig. 2). Such behaviour testifies to lowering the longitudinal compressibility and strength of the nanocomposites.

The Poisson's ratio increases as the tensile strength decreases and $P(0.01)/P(0) \approx \nu(0.01)/\nu(0) = 1.2$. Increasing ν is mainly due to that the epoxy becomes more pliable to transverse strain as the loading increases. Therefore, the FLG epoxy nanocomposites are an anisotropic polymer system. Their anisotropy may be related by weak coupling between the resin chains and basal plains of FLG plates and strong binding of the chains to free carbon bonds on lateral surfaces of FLG plates.

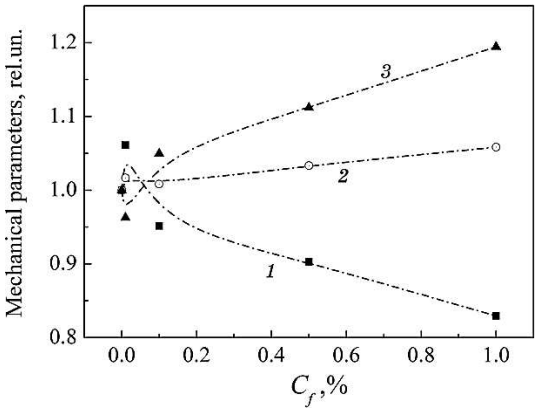

Fig. 2. The loading dependences of the static mechanical parameters of FLG epoxy nanocomposites—the tensile strength on compression (*1*), the Young's modulus (*2*), and the Poisson's ratio (*3*).

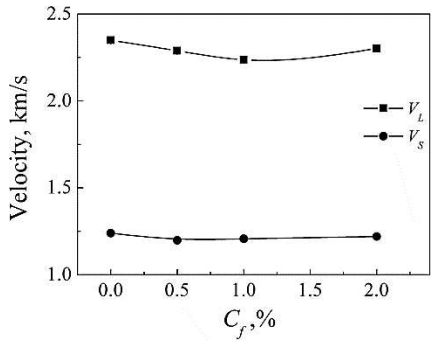

Fig. 3. The loading dependences of the longitudinal (V_L) and shear (V_S) elastic-wave phase velocities measured in the FLG-filled nanocomposites based on the ED-20 epoxy resin.

3.2. The Ultrasound-Velocity Measurements

The loading dependences of the longitudinal (V_L) and shear (V_S) elastic-wave phase velocities measured in the FLG epoxy nanocomposites are shown on Fig. 3. It is seen that the V_L demonstrates a weak nonmonotonic behaviour within the interval of $C_f < 2.0\%$ where it reaches its minimal values near $C_f = 1.0\%$ whereas variations in the V_S are small.

Very small decrements in both the velocities testify to negligible decrements in the elastic modules of FLG epoxy nanocomposites (namely, the Lame constant, the shear modulus, the compression modulus, the Young's modulus, and the Poisson's ratio).

3.3. The Thermal Resistivity

Figure 4 shows the thermal decomposition spectrum for the unfilled epoxy resin (Fig. 4, *a*) and its FLG-filled nanocomposites (Fig. 4, *b*, *c*, *d*). No new lines emerge in the correspondent spectra when embedding the FLG plates into the resin (Fig. 4, *b*). However, line intensities vary strongly with increasing the filler loading.

The majority of lines observed in the spectra can easily be identified by looking on the epoxy structural formula. In the range of $15 \le m/z \le 18$, desorption of the methyl groups CH_3 (15), the hydroxyl groups OH (17), and the water molecules H_2O (18) occur. In the range of $27 \le m/z \le 31$, intensive lines are related to the vinyl group $CHCH_2$ (27), the carbon monoxide CO (28), the carbonyl group COH (29), OCH_2 (30), and CH_2OH (31). The fragments of the epoxy chains, namely $(CH)_3$ (39), $CHCH_2CH$ (40), CH_2CO (42), CH_3CO (43), CH_2OCH (43), CH_2OCH_2 (44), $CHCH_2OH$ (44), $OHCHCH_3$ (45), the carboxyl group

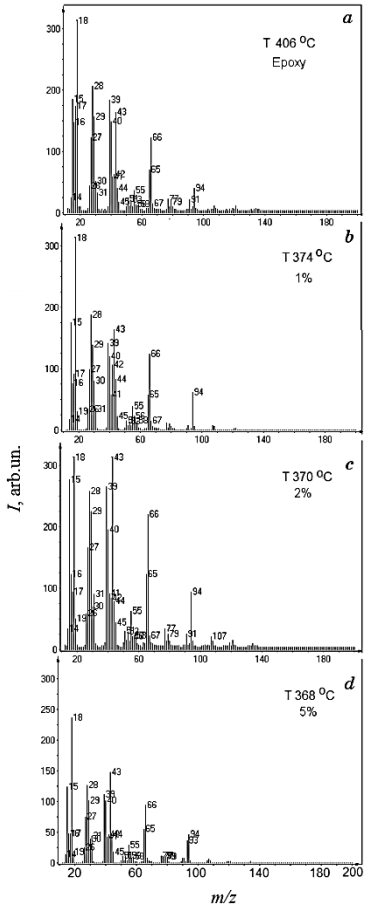

Fig. 4. The thermal decomposition spectra for the unfilled epoxy resin (*a*) and its FLG-filled nanocomposites of $C_f = 1\%$ (*b*), 2% (*c*), and 5% (*d*).

COOH (45) appear in the m/z ranges of 39–45. Finally, the fragments of COOCH (57), CH_2COHCH_2 (57), $(CH_2)_2CHOH$ (58), $COOCH_3$ (59), $CH_3CHOHCH_2$ (59), $CHCHCH_2CHCH$ (66) appear in the m/z ranges of 57–66. The other light fragments, such as of $m/z = 16$, 41, 55, 65 may be related to nitrogen-containing additives introduced into the neat resin together with the hardener. Finally, more heavy fragments contain the benzene ring residue, for example, C_6H_5 (77) and $C_6H_4CH_3$ (94).

Figure 5 shows a few sets of the thermal decomposition curves for the unfilled epoxy resin and its FLG-filled nanocomposites for the fragments of $m/z = 15$, 17, 28, 30.

One can see that the FLG plates cause a lowering in composites' line intensities as compared to the unfilled resin. The lowering is seemed to occur due to chemical binding of the unlinked chain segments to free

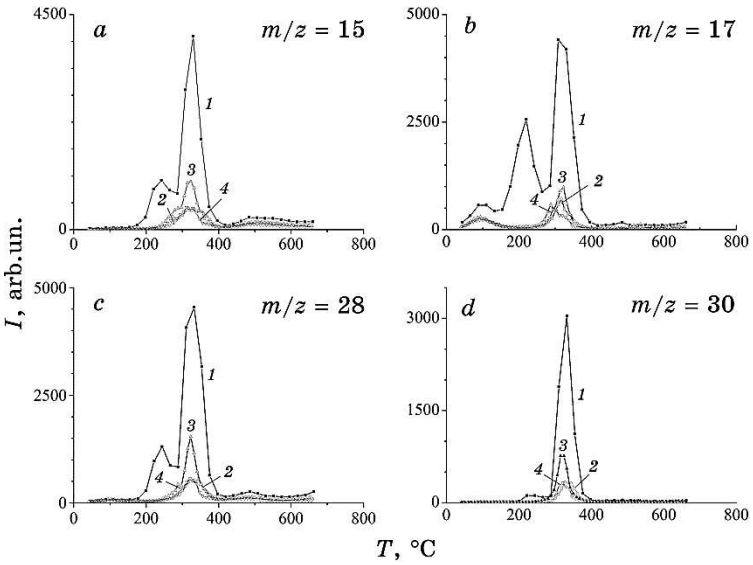

Fig. 5. The thermal decomposition curves for the unfilled epoxy resin (the curves '1') and its FLG-filled nanocomposites of $C_f = 1\%$ (the curves '2'), 2% (the curves '3'), and 5% (the curves '4') for the fragments of $m/z = 15$ (*a*), 17 (*b*), 28 (*c*), 30 (*d*).

carbon bonds located on the verges of FLG plates. This process can be treated as oxidation of the edge carbon bonds by small chain moieties, such as CH_3, OH, COO, H_2CO, and others. The binding, in turn, results in increasing activation energies for the correspondent segments and, hence, in lowering the chain mobility. Thus, the FLG plates promote an essential improvement in the thermal resistivity of the epoxy resin. Increasing the thermal resistivity of the FLG-filled nanocomposites can be related with stabilization of the resin 3*D*-network structure and lowering the epoxy chain mobility due to binding the chains to the lateral surface of the FLG particles and a denser 3*D*-network near the plate verges.

It is clear that increasing the Young's modulus (see Fig. 2) is also due to the graphene-chain binding. At the same time, the tensile strength lowers. It may be suggested that chain-graphene interaction is weakened in the vicinity of the graphene plates. By other words, the resin 3*D*-network is stabilized near the graphene plate verges whereas it is violated (*i.e.*, it is less dense) over the planes. The weakly coupled resin areas cause the tensile strength to lower.

In addition, the FLG plates block the heat propagation across their planes, take a heat away from the vibrating chains coupled to the plates, and dissipate the heat. Such the mechanism results in lowering the chain vibration amplitude and increasing the thermal

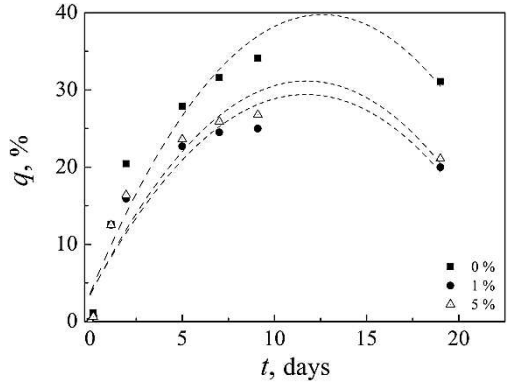

Fig. 6. Time dependences of the swell index (q) for the unfilled epoxy resin (0%) and its FLG-filled nanocomposites.

resistivity of the composites. However, the resistivity increases nonmonotonically with increasing loading. Indeed, the resistivity decreases at $C_f > 1\%$ and begin to grow again at $C_f > 2\%$. Since the thermal resistivity is related to the durability of the 3D-network structure, the latter has to vary nonmonotonically with increasing loading too.

3.4. Chemical Swelling

To confirm nonmonotonic variations in the resin 3D-network structure under loading it with the FLG plates, the swelling technique have been applied.

Time dependences of the swell index (q) for the unfilled resin (0%) and its FLG-filled nanocomposites with filler content of 1 and 5% are presented in Fig. 6. The swelling curves are typical for a case of the relaxation processes that show up after 10 days of staying in the solvent. Since the swelling index decreases with the loading, it testifies to increasing the chemical resistivity of the nanocomposites.

The time dependences of the swell index at $t \le 10$ days can be approximated by exponents and the fact evidences on a diffusion character of behaviour of q versus t during this period. In addition, Figure 6 shows a nonmonotonic dependence of q on the loading. Lowering q with increasing loading may indicate a tightening of the 3D-network in the vicinity of FLG plates and, on the other hand, a restriction in mobility of unlinked segments of resin chains due to binding them to lateral verges of FLG plates. The nonmonotonic dependence of q versus loading correlates with the loading dependence of the thermal resistivity.

4. CONCLUSIONS

It has been shown by using the PTDMS technique that the thermal resistivity of FLG-filled nanocomposites based on the ED-20 epoxy resin increases nonmonotonically at $C_f \leq 5\%$. The effect is caused by chemical binding of unlinked segments of the macromolecular chains to the free carbon bonds located on the verges of FLG plates and their anisotropic chemical properties.

The data obtained by using the SML technique reveal that the tensile strength of the nanocomposites increases at low loadings ($C_f \leq 0.01\%$) and decreases with increasing the loading whereas the Young's modulus increases gradually over the entire loading region ($C_f \leq 5\%$). The shear and longitudinal phase velocities show very small variations with increasing loading and, thus, testify to small variations in the dynamic elastic modules of FLG-filled nanocomposites.

Swelling of FLG-filled nanocomposites being embedded into the polygraph solvent weakens with increasing the loading. The effect specifies on that the FLG plates improve the chemical resistivity of the epoxy resin.

REFERENCES

1. K. M. F. Shahil and A. A. Balandin, *11-th IEEE Conference on Nanotechnology (August 15 18, 2011, Portland)* (Portland: 2011), p. 1193.
2. H. Kim, A. A. Abdala, and C. W. Macosko, *Macromolecules*, **43**: 6515 (2010).
3. C. D. Reddy, S. Rajendran, and K. M. Liew, *Nanotechnology*, **17**: 864 (2006).
4. D. W. Boukhvalov, M. I. Katsnelson, and A. I. Lichtenstein, *Phys. Rev. B*, **77**: 035427/1 (2008).
5. P. L. Andres, R. Ramírez, and J. A. Vergés, *Phys. Rev. B*, **77**: 045403/1 (2008).
6. A. A. Balandin, S. Ghosh, W. Bao et al., *Nano Lett.*, **8**: 902 (2008).
7. S. Ghosh, I. Calizo, D. Teweldebrhan et al., *Appl. Phys. Lett.*, **92**: 151911 (2008).
8. E. Pop, D. Mann, Q. Wang, K. Goodson, and H. Dai, *Nano Lett.*, **6**: 96 (2006).
9. M. S. Dresselhaus, G. Dresselhaus, and P. C. Eklund, *Science of Fullerenes and Carbon Nanotubes* (New York: Academic Press: 1996).
10. C. Faugeras, B. Faugeras, M. Orlita et al., *ACS Nano*, **4**: 1889 (2010).
11. Z. Y. Xia, S. Pezzini, E. Treossi et al., *Adv. Funct. Mater.*, **23**: 4684 (2013).
12. A. K. Geim and K. S. Novoselov, *Nature Materials*, **6**: 183 (2007).
13. M. Bratychak, O. Ivashkiv, and O. Astakhova, *Dopovidi Nats. Akad. Nauk Ukrainy*, **8**: 97 (2014) (in Ukrainian).
14. G. V. Kozlov and D. S. Sanditov, *Angarmonicheskie Effekty i Fiziko-Mekhanicheskie Svoistva Polimerov* [Anharmonic Effects and

Physicomechanical Properties of Polymers] (Novosibirsk: Nauka: 1994) (in Russian).
15. D. Royer, and E. Dieulesaint, *Elastic Waves in Solids I: Free and Guided Propagation* (New York: Springer: 2000).
16. B. M. Gorelov, A. M. Gorb, O.I. Polovina et al., *J. Appl. Phys.*, **112**: 094321/1 (2012).
17. V. A. Pokrovsky, *J. Therm. Anal. Cal.*, **62**: 407 (2000).
18. V. A. Pokrovsky, *Surface*, **17**: 63 (2010).